

Development of a novel self-centering buckling-restrained brace with BFRP composite tendons

Z. Zhou^{*}, X.T. He^a, J. Wu^b, C.L. Wang^c and S.P. Meng^d

Southeast University, Key Laboratory of Concrete and Prestressed Concrete Structures of the Ministry of Education, Nanjing, 210096, China

(Received May 09, 2013, Revised October 01, 2013, Accepted December 30, 2013)

Abstract. Buckling-restrained braces (BRBs) have excellent hysteretic behavior while buckling-restrained braced frames (BRBFs) are susceptible to residual lateral deformations. To address this drawback, a novel self-centering (SC) BRB with Basalt fiber reinforced polymer (BFRP) composite tendons is presented in this work. The configuration and mechanics of proposed BFRP-SC-BRBs are first discussed. Then an 1840-mm-long BFRP-SC-BRB specimen is fabricated and tested to verify its hysteric and self-centering performance. The tested specimen has an expected flag-shaped hysteresis character, showing a distinct self-centering tendency. During the test, the residual deformation of the specimen is only about 0.6 mm. The gap between anchorage plates and welding ends of bracing tubes performs as expected with the maximum opening value 6 mm when brace is in compression. The OpenSEES software is employed to conduct numerical analysis. Experiment results are used to validate the modeling methodology. Then the proposed numerical model is used to evaluate the influence of initial prestress, tendon diameter and core plate thickness on the performance of BFRP-SC-BRBs. Results show that both the increase of initial prestress and tendon diameters can obviously improve the self-centering effect of BFRP-SC-BRBs. With the increase of core plate thickness, the energy dissipation is improved while the residual deformation is generated when the core plate strength exceeds initial prestress force.

Keywords: seismic design; self-centering; buckling-restrained brace; residual deformation; hysteric response; composite tendon

1. Introduction

A buckling-restrained brace (BRB) has been verified as a good seismic-resisting structural component with excellent hysteretic behavior (Tsai *et al.* 2004, Fahnestock *et al.* 2007, Park *et al.* 2012, Wang *et al.* 2012, Wu *et al.* 2012). Usually, a BRB mainly consists of two basic components: a steel core element that bears the entire axial load of brace and a restraining element that prevent the core element from buckling in compression. Under a minor and moderate seismic excitation,

*Corresponding author, Associate Professor, E-mail: seuhj@163.com

^a M.S., E-mail: tonr_he@qq.com

^b Professor, E-mail: wujing@vip.sina.com

^c Ph.D., E-mail: chunlin@seu.edu.cn

^d Professor, E-mail: cardoso_meng@sina.com

BRBs keep elastic and work as an effective lateral force resisting component to ensure the stiffness requirement and normal use of main structures. When a strong seismic excitation happens, the core of BRBs would yield in both tension and compression to dissipate most energy in earthquake. As a result, responses of main structure can be reduced rapidly. Therefore, BRBs are considered as replaceable fuses in a seismic-resisting structural system. In the last few years, buckling-restrained braced frames (BRBFs) have been used extensively in some North American and Asian countries and areas.

Despite BRBs have satisfactory seismic performance and can be easily replaced after earthquake, BRBFs are still susceptible to residual lateral deformations over the building height due to the low post-yield stiffness of BRBs. The residual story drifts can reach on average 40%-60% of the maximum drifts (Sabelli *et al.* 2003). This problem may greatly increase repair difficulties and costs after significant seismic event, unless the BRBF is backed up by a moment-resisting frame to reduce its residual deformations (Kiggins and Uang 2006). To address this drawback, an effective way is to introduce a self-centering (SC) system into BRBs, which has the ability to dissipate energy and also return to their original position after ground shaking. Most researches regarding SC systems have been focused on applying post-tensioning (PT) technology in beam-column connections or rocking systems to generate gap opening in specified locations (Garlock *et al.* 2005, 2007). These will bring great challenges associated with connection to the gravity system and transfer of inertial forces. However, SC braces lack these challenges and obtain more and more attention recently. Christopoulos *et al.* (2008) developed a SC brace using PT high-strain-capacity aramid-fiber tendons to clamp the brace together. Two steel tubes and one tensioning element sets are used to produce stable self-centering force. The energy dissipation is generated through friction interface. Chou *et al.* (2012) proposed a steel dual-core SC brace with a flag-shaped re-centering hysteretic response under cyclic loads. In this way, axial deformation capacity of the brace is doubled by serial deformations of two sets of tensioning elements arranged in parallel. Some studies also considered using shape memory alloys (SMA) to develop SC braces with both self-centering force and energy dissipation (Dolce and Cardone 2006, Zhu and Zhang 2008, Miller *et al.* 2011). However, SMA is expensive to construct and also difficult to meet requirements of different design forces in civil engineering.

Basalt fiber reinforced polymer (BFRP) is a kind of recently developed composite polymer materials which can be used in civil structures. It has more sufficient elongation capacity than high-strength steel strands and lower economic cost than Aramid or Carbon FRP. By introducing the PT-SC system into BRBs, this paper proposes a novel steel self-centering buckling-restrained brace (SC-BRB) with BFRP composite tendons. A BFRP-SC-BRB consists of steel core elements for energy dissipation, composite tendons for producing self-centering forces, steel tubes to restrain buckling of core elements and make tendons elongate in earthquake. The configuration and mechanics of BFRP-SC-BRBs are first discussed. Then an 1840-mm long BFRP-SC-BRB is fabricated and tested to verify its hysteric and self-centering performance. Additionally, numerical parametric analysis are conducted by using OpenSEES software to evaluate the influence of initial prestress, tendon diameter and core plate thickness on the performance of BFRP-SC-BRBs.

2. Configuration and mechanics of BFRP-SC-BRB

2.1 Configuration of BFRP-SC-BRB

Fig. 1 shows the configuration details of a proposed BFRP-SC-BRB, which mainly consists of

two steel energy-dissipative core plates, two steel bracing tubes (inner tube and outer tube), four PT-BFRP composite tendons and two anchorage plates. Fig. 1(a) shows the overall view of the whole brace. Fig. 1(b) is the cross section view of Fig. 1(a) (Section 1 and Section 2), including BFRP tendons, inner tube, core plates, filler plates and outer tube from inside to outside. Fig. 1(c) shows the planar location of core plates, which are welded to the inner tube at left end and outer tube at right end.

Core plates have the same length with the whole brace, which can be divided into the energy-dissipative yielding segment and non-yielding connection segment along length direction (shown in Fig. 1(c)). They are laid between surfaces of inner and outer tube. The energy-dissipative segment is slotted to assure it can yield. Filler plates are used to prevent energy-dissipative segment from in-plane instability. Out-plane buckling of energy-dissipative segment is restrained by two bracing tubes (shown in Fig. 1(b)), making the whole brace has stable hysteric performance in earthquake.

The SC system is composed of steel bracing tubes, post-tensioned BFRP tendons, and anchorage plates. The inner tube is welded to the left end of core plates (shown in Fig. 1(c)) and remains fixed with respect to the left end connection. The outer tube is welded to the right end of core plates and remains fixed with respect to the right end connection. Anchorage plates have slots (shown in Fig. 1(a)) through which core plates can pass. It should be noticed that anchorage plates are not connected to core plates or to tubes, allowing them to slide freely along core plates. BFRP tendons are tensioned and anchored to anchorage plates against the inner and outer tubes, creating an initial compression in these two bracing tubes.

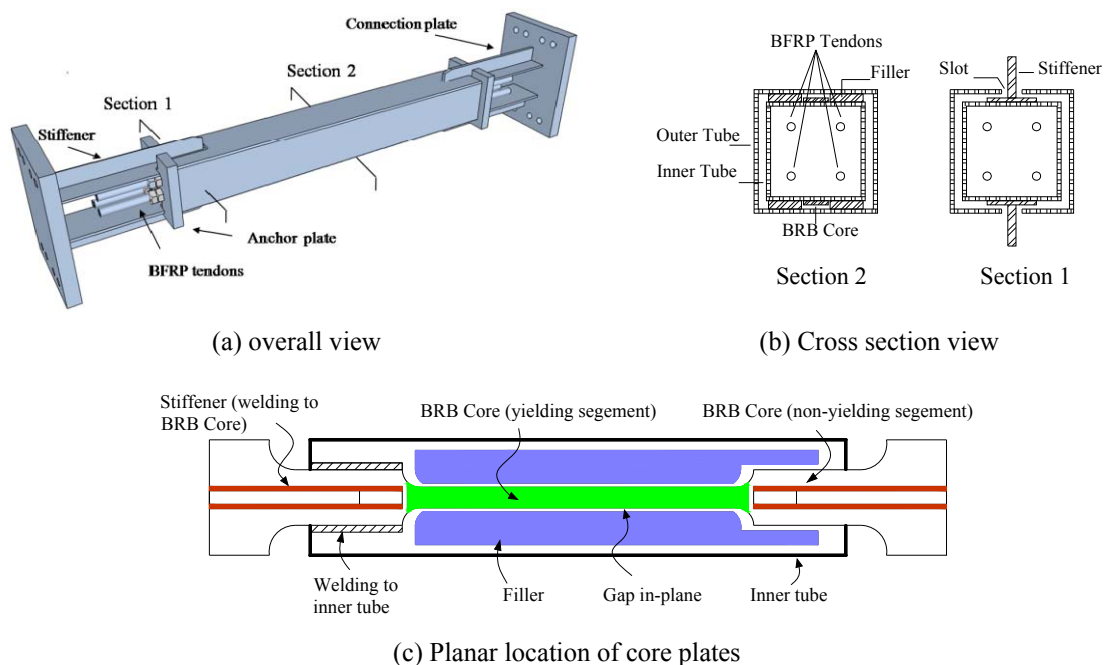


Fig. 1 Configuration details of a proposed BFRP-SC-BRB

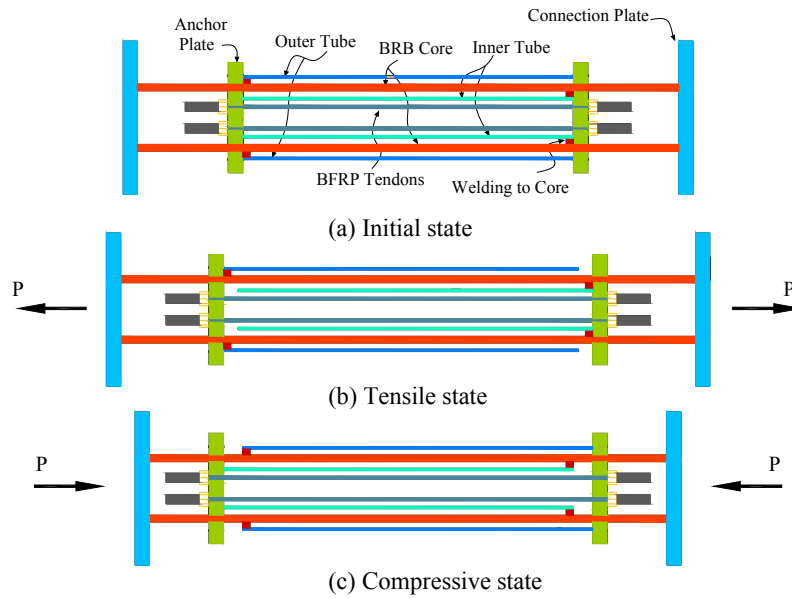


Fig. 2 Working mechanism of a BFRP-SC-BRB

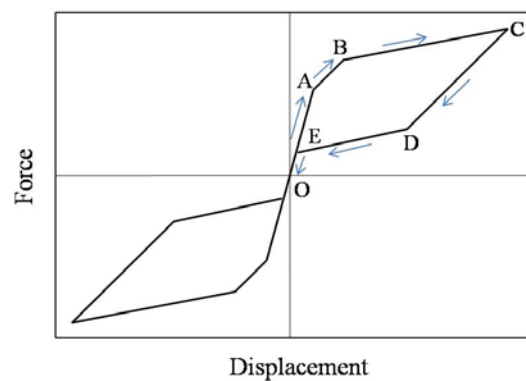


Fig. 3 Expected force-displacement response of BFRP-SC-BRBs

2.2 Working mechanism of BFRP-SC-BRB

Fig. 2 shows the working mechanism of BFRP-SC-BRBs. As shown in Fig. 2(a), before brace subjects to external force, both ends of bracing tubes are clamped by anchorage plates through the prestress in BFRP tendons. This is the initial state of the brace. If the brace has a self-centering ability, it should resume to the location of initial state in unloading state. This can be achieved by the self-centering force in BFRP tendons. To ensure the tendons are always stretched in earthquake, the inner and outer tubes act as struts to push the anchorage plates apart. When brace is in tension (Fig. 2(b)), the inner tube pushes the left anchorage plate and the outer tube pushes the right

anchorage plate to make them move apart, leading to an extra elongation of BFRP tendons. The tendons have a trend to resume their original length. Then a restoring force is produced in brace and self-centering is achieved. When brace is in compression (Fig. 2(c)) the inner tube pushes the right plate and the outer tube pushes the left anchorage plate. At this time, the two anchorage plates also move apart, resulting in additional tendon elongation and increasing self-centering force. Although the core plates could yield and then have plastic deformation in earthquake, the components of SC system (tendons, inner tube and outer tube) remain in elastic range. The self-centering force (prestress plus increased tensile force) will make the SC system resume to their original location in the initial state. Then, core plates will also be driven to overcome the plastic deformation and resume to their original length, since they are welded to the inner and outer tube. In this way, the proposed BFRP-SC-BRB can achieve self-centering ability in both tension and compression.

2.3 Stiffness analysis of BFRP-SC-BRB

Fig. 3 shows the expected force-displacement response of BFRP-SC-BRBs. Stiffness of the brace changes in different deformation stages. In a tensile (compressive) process, this can be basically divided into six stages as follows:

(1) Stage I: OA

In this stage, the external load is less than the prestress in tendons. As a result, the brace would not be activated. Core plates, BFRP tendons and bracing tubes deform coordinately until tubes separate from anchorage plates. The axial stiffness of the brace in this stage, K_1 , is the maximum and can be expressed as

$$K_1 = k_{in} + k_{ou} + k_b + k_c \quad (1)$$

Where k_{in} and k_{ou} are the axial stiffness of the inner and outer tube respectively; k_b is the axial stiffness of BFRP tendons; k_c is the axial stiffness of core plates.

(2) Stage II: AB

When external load exceeds the prestress in tendons, the brace is activated. At this time, the initial compressive force in bracing tubes disappears; BFRP tendons and core plates are elastically stretched until core plates yield. The axial stiffness of the brace in this stage, K_2 , can be expressed as

$$K_2 = k_b + k_c \quad (2)$$

(3) Stage III: BC

After core plates yield, the axial stiffness of the brace decreases distinctly and the brace deformation increase rapidly, resulting from a low post-yield stiffness of steel core plates. However, the tendons still keep in elastic range. The axial stiffness of the brace in this stage, K_3 , can be expressed as

$$K_3 = k_b + \alpha k_c \quad (3)$$

Where α is a coefficient to account for the post-yield stiffness of core plates.

(4) Stage IV: CD

When brace deforms to a target value, it begins to be unloaded. At this time, core plates resume

their initial elastic stiffness and work coordinately with BFRP tendons. As a result, the axial stiffness of the brace in this stage is similar with that in Stage II.

(5) Stage V: DE

In this stage, core plates yield in compression. BFRP tendons are still in elastic range and providing self-centering force for the whole brace. As a result, the axial stiffness of the brace in this stage is similar with that in Stage III.

(6) Stage VI: EO

The last stage in unloading process begins when the bracing tubes contact anchorage plates. The stiffness in this stage is similar with that in Stage I while the deformation process is opposite. At the end of this stage, the brace will return to its original position.

3. Quasi-static test of a BFRP-SC-BRB

3.1 Design of the specimen

In the performance-based seismic design methodology, braces should have sufficient deformation rate capacity. According to the AISC Seismic Provisions, BRBs are required to work normally under a major earthquake in which the inter-story drift of braced frames reaches 2%. Fig. 4 shows the deformation of a braced frame. The inter-story drift, Δ_c , can be determined as

$$\Delta_c = 0.02h \quad (4)$$

Where h is the storey height of brace frames. The ratio of core plate length to total brace length, r , is defined as

$$r = l_c / l_0 \quad (5)$$

Then, the deformation rate demand of BFRP-SC-BRBs, ζ , can be obtained as

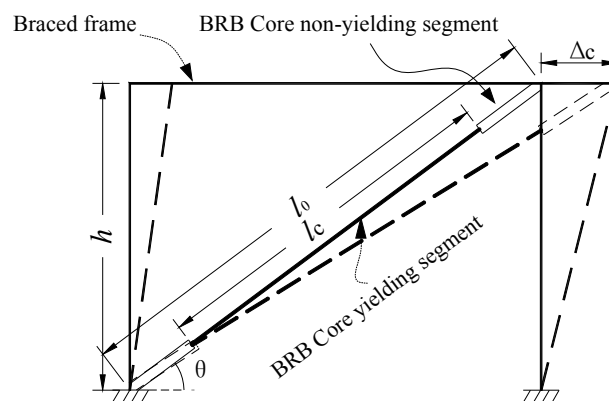


Fig. 4 Deformation of a braced frame

$$\zeta = \frac{0.2h \cos \theta}{h / \sin \theta} = \frac{\sin \theta \cos \theta}{50r} \quad (6)$$

Where θ is the inclination of the brace.

To ensure BFRP-SC-BRBs self-centering, the initial prestress force in BFRP tendons, F_p , should be greater than the maximum strength of core plates, F_{yc}

$$F_p = p_B A_B \geq F_{yc} = \beta \phi f_y A \quad (7)$$

Where ϕ is the strain hardening factor for core plates; β is the compression strength factor for core plates; p_B is the initial stress in tendons; A_B is the total area of BFRP tendons; f_y is the yield stress of core plates; A is the total area of core plates.

Then, the design capacity of the BFRP-SC-BRB can be calculated as follows

$$F_u = F_{yc} + F_p = \beta \phi f_y A_c + p_B A_B \quad (8)$$

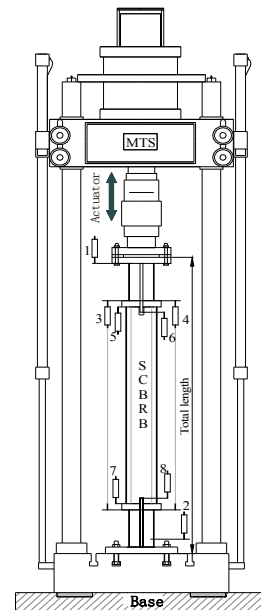
According to Eqs. (1)-(8), a specimen can be designed for the quasi-static test. The material properties of steel and BFRP tendon used in the specimen are tested and measured before fabrication. The total length of the BFRP-SC-BRB specimen is determined as 1840 mm. The length of core plates is 890 mm. The effective length of BFRP tendons is 1200 mm. The inclination of the brace in a frame structure is set as 30°. The deformation rate demand is computed as 0.87% for total brace length and 1.79% for core plate length. In actual engineering, the length of core plates is much larger than connecting length. So the actual deformation rate demand of BFRP-SC-BRBs is closer to the former one. In this test, the controlled deformation rate is set as 1.0%. The section of core plates is set as 34 × 7.5 mm. The material of core plates is Q235 with the elastic modulus 213 GPa and yield strength 277 MPa. Four 14-mm-diameter BFRP tendons are used in this specimen with the elastic modulus 48 GPa and ultimate strain 2.4%. The initial prestress in BFRP tendons is computed as 325MPa. The sections of inner and outer tube are determined as HSS 120 × 120 × 7.5 mm and HSS 210 × 210 × 12 mm respectively. All the components of the specimen are assembled and welded in a factory. The anchorage plates are spot-welded to the two ends of inner tube. Then BFRP tendons are pulled through the inner tube and anchored to anchorage plates. Core plates are assembled passing through the slots of anchorage plates and then welded to the inner tube. Filler plates are horizontally arranged at the sides of core plates to provide lateral supports for the in-plane stability of core plates. The outer tube is then assembled and welded.

3.2 Test results

Fig. 5 shows the specimen on a testing machine. Fig. 5(a) is a specimen testing photo and Fig. 5(b) is a diagram of specimen and testing machine. The specimen is subjected to a cyclic loading test of displacement control with increasing amplitude (Fig. 6). Displacement gages (highlighted by number 1-7 in Fig. 5(b)) are employed to measure the displacement of two anchorage plates and welded ends of bracing tubes. Gage 1 and 2 are set to measure the displacement of two connection plates. Gage 3 and 4 are both used to measure the relative displacement between two anchorage plates. Gage 6 and 8 are employed to measure the displacement at welding end of inner tube and outer tube, respectively. Gage 5 and 7 are used to measure the displacement of upper and



(a) Apecimen testing photo



(b) Diagram of specimen and testing machine

Fig. 5 Specimen on a testing machine

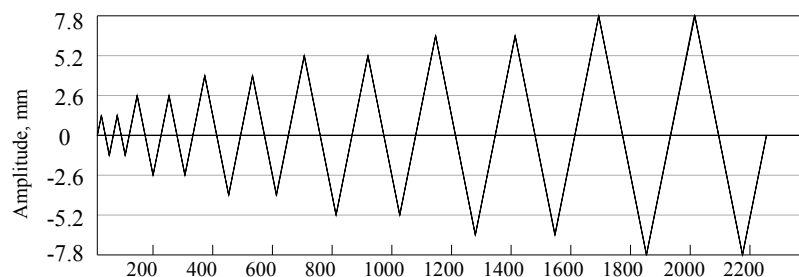


Fig. 6 Loading protocol

lower anchorage plate, respectively. Then the total brace deformation can be computed by the displacement difference of gage 1 and 2. The BFRP tendon elongation is determined by averaging the displacements of gage 3 and 4. The displacement difference of gage 5 and 6 is used to compute the gap between the welding end of inner tube and end plate, The gap value between the end plate and welding end of outer tube is determined by the displacement difference of gage 7 and gage 8.

It can be seen from Fig. 7 that the tested specimen has an expected flag-shaped hysteresis character, showing a distinct self-centering tendency. The residual deformation of the brace is only about 0.6 mm. The reason of the existence of this residual deformation may lies in two factors. First, the prestress loss may happen in BFRP tendons after pretensioned. The decrease of prestress has significant effect on the self-centering ability of BFRP-SC-BRBs, which will be detailedly discussed in Section 4. Moreover, some unexpected minor gaps may exist between components

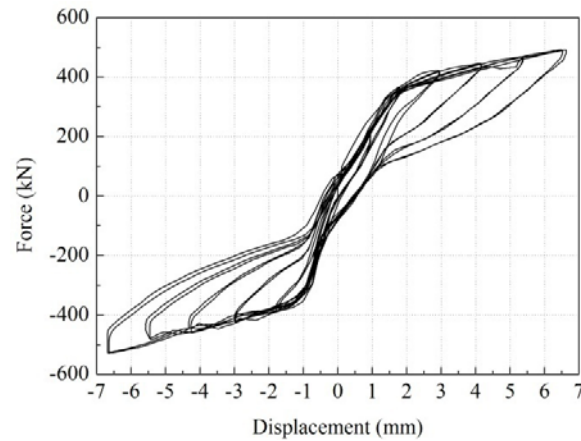


Fig. 7 Force-displacement response of the specimen

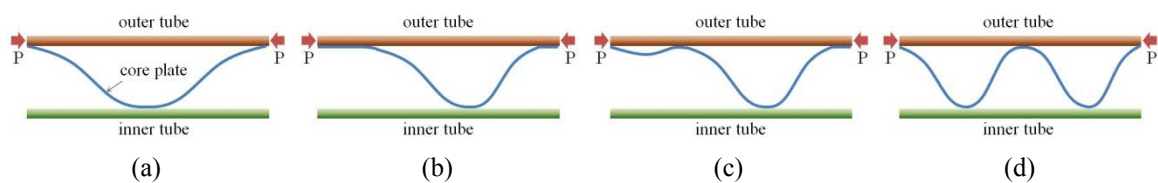


Fig. 8 Transition of compressive buckling wave

when fabricating and assembling the specimen in the factory. This will lead to an unrecoverable deformation during test. However, with the increase of loading amplitude, the residual deformation of the brace always keeps in the same level, indicating that the specimen has a stable self-centering ability.

Since the elastic deformation of connecting components, the measured displacement is less than the controlled loading amplitude. The maximum measured displacement in tension cycle is 6.63 mm while it is -6.68 mm in compression cycle. From Fig. 7, a little regular fluctuation in the compression cycle of force-deformation curve can be observed. The reason for this phenomenon is the change of compressive buckling wave. Fig. 8 shows the transition diagram of buckling wave. In Fig. 8(a), core plate buckles and has odd wave number at the beginning. With the increase of compressive load, the contact length between the core plate and restraining tube will increase (Fig. 8(b)). When the contact length is large enough, new buckling wave will be generated (Fig. 8(c)). At this time, without contacting restraining tube, the new buckling wave has not lateral support. Therefore, this state is unstable and it will rapidly transit into a more stable state in which the new buckling wave contact restraining tube (Fig. 8(d)). Therefore, in the process from Fig. 8(c) to Fig. 8(d), the force in braces will have a sudden change. Thus a fluctuation in the force-displacement curve arises.

Fig. 9 shows the gap between bracing tubes and anchorage plates against overall brace displacement. When the brace is tensioned, the gap is close to zero since welded ends of bracing tubes attach to anchorage plates at this time. In compressive state, the gap begins to open and

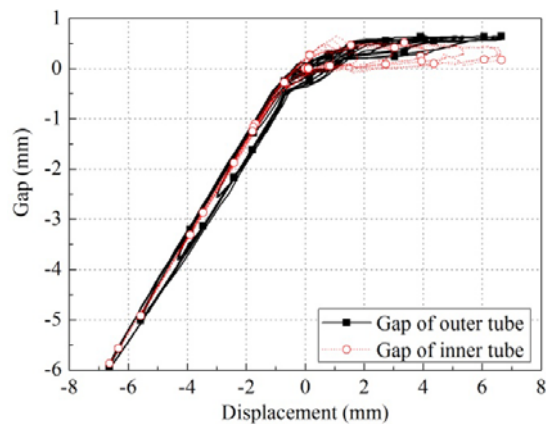


Fig. 9 Gap-displacement response of the specimen

becomes larger and larger with the increase of loading displacement. Whether in tension or compression, the gap of outer tubes is nearly the same with that of inner tubes. This indicates that the BFRP-SC-BRB works effectively during the test.

4. Numerical analysis

4.1 OpenSEES model for BFRP-SC-BRB

To conduct numerical analysis, the Open Source Earthquake Engineering Simulation (OpenSEES) software is used to model the nonlinear character of proposed BFRP-SC-BRBs (Mazzoni *et al.* 2009). In a numerical model, nonlinear beam-column elements are employed to simulate core plates. Truss elements are used for bracing tubes and BFRP tendons. Gap elements are used to simulate the contact behavior between bracing tubes and anchorage plates. All material properties for elements are from the test as shown in Section 3. Bilinear material model is used for core plates and bracing tubes. BFRP tendons are supposed as linear elastic material. The schematic diagram is shown in Fig. 10. The numbers in Fig. 10 denotes the numbering of nodes in the analysis model. Element 2-3 denotes the yielding segment of core plates, while element 1-2 and 3-4 are the non-yielding segments. Element 5-6 and 7-8 denotes outer and inner tube respectively. Element 9-10 and 11-12 denotes BFRP tendons. Element 9-13-14-11 and 10-15-16-12 denotes the anchorage plates.

4.2 OpenSEES model validation

In this section, two experiment results from other literatures (Christopoulos *et al.* 2008, Chou *et al.* 2012), and one experiment result from authors' own research (Section 3.2) are employed to validate the proposed OpenSEES model in Section 4.1. The experiments of Christopoulos *et al* and Chou *et al* are both on post-tensioned self-centering energy dissipative (PT-SCED) braces, in which a friction device is used to dissipate energy. Although this energy dissipative mechanism is

different from a buckling restrained brace, the self-centering system of PT-SCED braces is very similar to that of BFRP-SC-BRBs, mainly consisting of steel tubes and tensioning element sets. Therefore, the experiment results of PT-SCEDs can be used to validate the proposed OpenSEES modeling methodology for BFRP-SC-BRBs.

Christopoulos *et al.* (2008) tested the hysteric force-displacement response for a PT-SCED brace specimen. The brace has a length of 2170 mm. The interior tube was HSS254 × 254 × 8 mm and outer tube was HSS305 × 305 × 6.4 mm. The tensioning elements were comprised of four 17-mm-diameter Technora tendons. Four friction dissipative mechanisms were included. Their material model parameters were tested before the brace specimen was loaded. The experiment was finished at the University of Toronto Structures Laboratories. The proposed OpenSEES modeling methodology in Section 4.1 is used to conduct a numerical analysis for their brace. The simulation of self-centering components is the same with the model in Fig. 10. But the material model of BRB core plate needs to be changed to that of friction dissipative mechanisms. The analyzed responses are compared to the experiment result, as shown in Fig. 11. A relatively good agreement between the OpenSEES analysis and the experimental test can be observed.

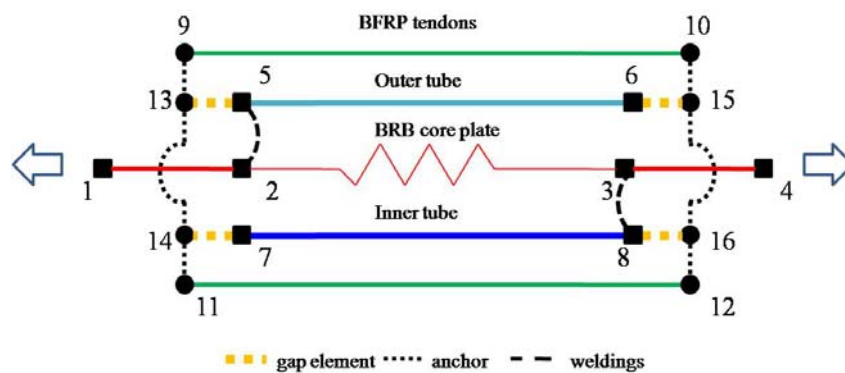


Fig. 10 Schematic diagram of OpenSEES model for BFRP-SC-BRB

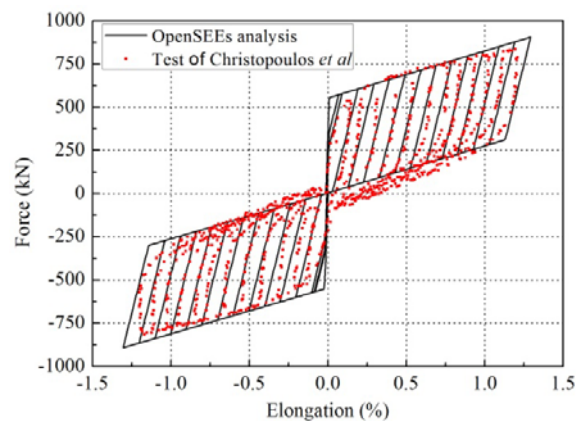


Fig. 11 Comparison between test of Christopoulos *et al.* (2008) and OpenSEES analysis

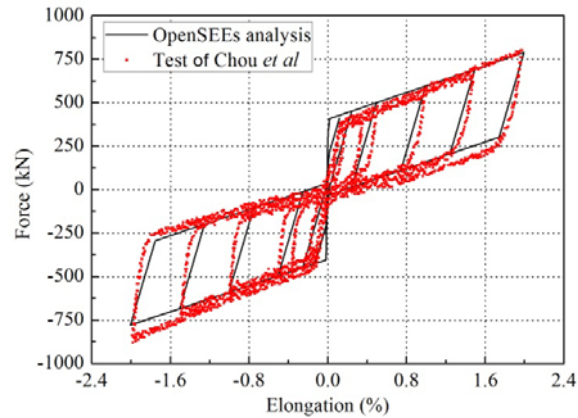
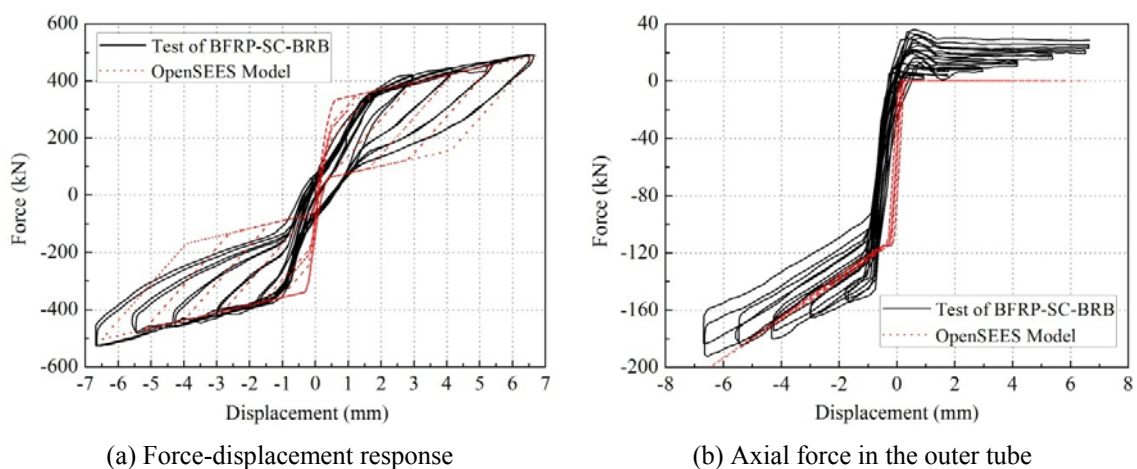


Fig. 12 Comparison between test of Chou *et al.* (2012) and OpenSEES analysis

Chou *et al.* (2012) tested a 5350-mm long dual-core PT-SCED to evaluate its cyclic performance. Compared to the previous work by Christopoulos *et al.* (2008), their brace adopted three tubes and two tensioning element sets of 22-mm diameter E-glass FRP tendons to reduce strain demands on the tensioning elements. But the self-centering and energy mechanism are still very similar to that of Christopoulos *et al.* (2008). The specimen is tested at the National Center for Research on Earthquake Engineering (NCREE), Taiwan. The proposed OpenSEES modeling methodology in this paper is employed to conduct numerical analysis. The predicted results and experiment result are compared in Fig. 12. A relatively good agreement between the OpenSEES analysis and experimental test can be still observed.

Fig. 13 shows the comparison between the predicted responses of proposed OpenSEES model (Fig. 10) and authors' own experiment results (Section 3.2). It can be seen that the



(a) Force-displacement response

(b) Axial force in the outer tube

Fig. 13 Comparison between the test of BFRP-SC-BRB and numerical analysis results

force-displacement curves of them are similar. Both simulated maximum tension and compression forces are very close to test results. Since the prestress loss and unexpected small component gaps are not considered in numerical model, an ideal self-centering result is achieved in numerical analysis with the residual brace deformation is zero. As for the axial force in the outer tube, numerical analysis has the same changing tendency with test results. In each stressing state, the curve slope of numerical analysis and test results are similar.

4.3 Parametric investigation

The validation results in Section 4.2 show a relatively good agreement between OpenSEES simulation and experimental test. The proposed OpenSEES model can simulate the gap opening at the end of bracing tubes and tendon elongation induced by pushing anchorage plates. As a result, the self-centering mechanism can be simulated accurately enough. Among the three validations, the difference between the response curve shape of simulation and test is a little larger for the BFRP-SC-BRB specimen. The reason lies in the energy dissipating mechanism of BRB is more complicated than that of friction device. Although the plastic energy dissipation of steel core plates is included in the OpenSEES model for BFRP-SC-BRBs, it still has two limitations. First, a simplified bilinear material model is used for steel core plates. Sometimes it is not accurate enough to describe the nonlinear behavior of steel material in cyclic loading. Moreover, for a real BFRP-SC-BRB, the core plate would buckle in compression and then contact and rub inner and outer tube. This could have some influence on the energy dissipating of core plate in compression, while can not be simulated in the proposed OpenSEES model. However, the proposed model can still simulate the main hysteric behavior of BFRP-SC-BRBs to a large extent. The parametric investigation results based on this model can still reflect the influence of the key parameters on the brace performance.

To investigate factors influencing the self-centering effect of BFRP-SC-BRBs, three parameters are considered to be changed in the OpenSEES model, including initial prestress in tendons, tendon diameter and core plate thickness (Table 1). The characters (P, D and T) of model ID stand for the initial prestress, tendon diameter and core plate thickness respectively. The numbers in model ID after each character identify their actual values in the numerical analysis.

Figs. 14-16 show the effect of investigated parameters on force-displacement responses of BFRP-SC-BRBs. It can be seen from Fig. 14 that with the increase of initial prestress in tendons,

Table 1 Parametric investigation scheme

Model numbering		Initial prestress in tendons (MPa)	Diameter of tendons (mm)	Core plate thickness (mm)
No.	ID			
1	P250D12T7.5	250	12	7.5
2	P325D12T7.5	325	12	7.5
3	P400D12T7.5	400	12	7.5
5	P250D14T7.5	250	14	7.5
6	P250D16T7.5	250	16	7.5
7	P250D14T5.0	250	14	5.0
8	P250D14T10.0	250	14	10.0

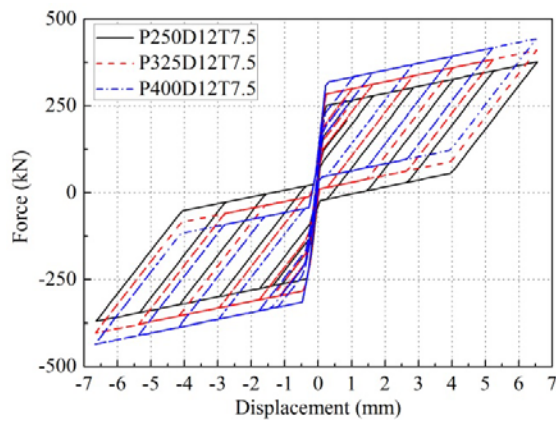


Fig. 14 Effect of initial prestress force on BFRP-SC-BRB responses

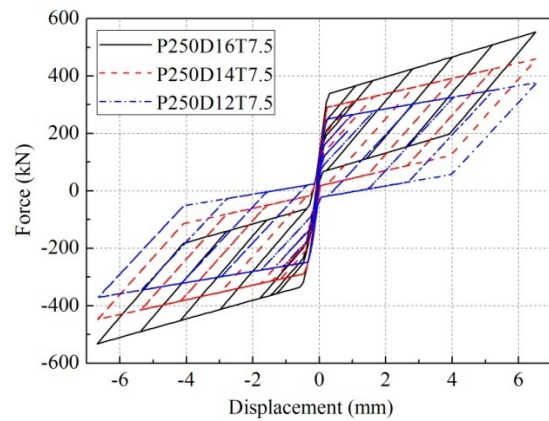


Fig. 15 Effect of tendon diameter force on BFRP-SC-BRB responses

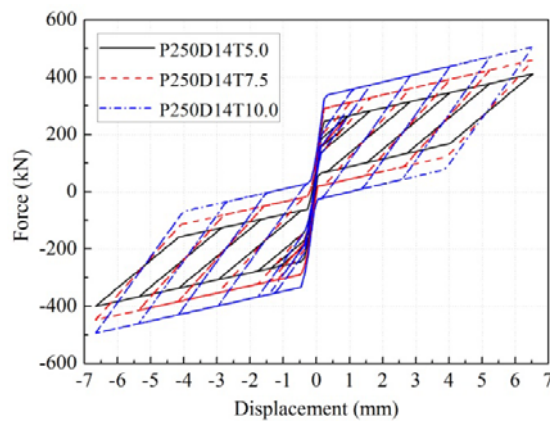


Fig. 16 Effect of core plate thickness on BFRP-SC-BRB responses

the self-centering ability of the brace is distinctly improved, and the maximum brace force is also enhanced. When prestress is insufficient, BFRP-SC-BRBs cannot be totally self-centered and some residual brace deformation will be kept. The slopes of force-displacement curves are the same under different initial prestress cases. This indicates that when tendon area is fixed, the change of initial prestress does not influence the stiffness of BFRP-SC-BRBs. Fig. 15 shows that the increase of tendon diameter can also obviously improve the self-centering ability of BFRP-SC-BRBs. This is because that the total prestress force is also enhanced. However, in this way, the brace stiffness will also be increased. Fig. 16 shows that with the increase of core plate thickness, the energy dissipation is improved while the self-centering ability decreases. When the core plate thickness is increased to make the core plate strength exceed the total initial prestress force, residual deformation will be generated in BFRP-SC-BRBs. It should be noticed that if a more accurate material model is used for steel core plates, the self-centering ability will decrease faster and more obviously with the increase of core plate thickness, for the strain hardening effect

of steel material in cyclic loading. Moreover, if the contact between core plates and bracing tubes can be modeled in numerical analysis, more accurate simulation results can be obtained through parametric analysis for the design of BFRP-SC-BRB components such as bracing tubes and core plates.

5. Conclusions

A novel steel self-centering buckling-restrained brace (SC-BRB) with Basalt fiber reinforced polymer (BFRP) composite tendons is presented in this work. It mainly consists of steel core plates, bracing tubes and BFRP tendons. Whether brace is in tension or compression, bracing tubes act as struts to make BFRP tendons elongated. As a result, proposed BFRP-SC-BRBs can achieve stable self-centering ability during earthquake. Quasi-static test results of an 1840-mm-long BFRP-SC-BRB specimen shows that the proposed BFRP-SC-BRB has an expected flag-shaped hysteresis character, showing a distinct self-centering tendency. The residual deformation of the tested specimen is only about 0.6 mm. The gap between anchorage plates and welding ends of bracing tubes performs as expected during the test, which is close to zero when brace is in tension while open and increase continuously in compressive state. The Open Source Earthquake Engineering Simulation (OpenSEES) software is employed to conduct numerical analysis. Experiment results are employed to validate the OpenSEES modeling methodology. A relatively good agreement is observed between numerical analysis and experimental measurements. Then a parametric investigation is conducted based on the proposed OpenSEES model. Results show that both the increase of initial prestress in tendons and tendon diameter can obviously improve the self-centering effect of BFRP-SC-BRBs. With the increase of core plate thickness, the energy dissipation is improved while a residual brace deformation is generated when the core plate strength exceed total initial prestress force.

Further studies are needed to conduct Quasi-static tests for more BFRP-SC-BRB specimens and even full-scale frames equipped with the proposed braces. A more accurate modeling methodology also needs further investigation to include more accurate material model for steel core plates and contact simulation between core plates and bracing tubes. Moreover, the influence of main configuration parameters on the seismic performance of BFRP-SC-BRB frames should be carefully studied to achieve more reasonable design procedures for BFRP-SC-BRB frames.

Acknowledgments

The research described in this paper was financially supported by “National Natural Science Foundation of China” (grant no. 51208095), “the Fundamental Research Funds for the Central Universities”, and “A Project Funded by the Priority Academic Program Development of Jiangsu Higher Education Institutions” (PAPD). The supports are gratefully acknowledged.

References

- Christopoulos, C., Tremblay, R., Kim, H.J. and Lacerte, M. (2008), “Self-Centering energy dissipative bracing system for the seismic resistance of structures: development and validation”, *J. Strut. Eng.*, **134**(1), 96-107.

- Chou, C.C., Chen, Y.C., Pham, D.H. and Truong, V.M. (2012), "Experimental and analytical validation of steel dual-core self-centering braces for seismic-resisting structures", *The 9th International Conference on Urban Earthquake Engineering*, Tokyo, March.
- Dolce, M. and Cardone, D. (2006), "Theoretical and experimental studies for the application of shape memory alloys in civil engineering", *J. Eng. Mater. Technol – T. ASME*, **128**(3), 302-311.
- Fahnestock, L.A., Sause, R. and Ricles, J.M. (2007), "Seismic response and performance of buckling-restrained braced frames", *J. Struct. Eng.*, **133**(9), 1195-1204.
- Garlock, M., Ricles, J.M. and Sause, R. (2005), "Experimental studies of full-scale post-tensioned steel connections", *J. Struct. Eng.*, **131**(3), 438-448.
- Kiggins, S. and Uang, C.M. (2006), "Reducing residual drift of buckling-restrained braced frames as a dual system", *Eng. Struct.*, **28**(11), 1525-1532.
- Garlock, M., Sause, R. and Ricles, J.M. (2007), "Behavior and design of posttensioned steel frame systems", *J. Struct. Eng.*, **133**(3), 389-399.
- Mazzoni S., McKenna F., Scott M.H. and Fenves G.L. (2009), Open system for earthquake engineering simulation (OpenSees), User command language manual, Pacific Earthquake Engineering Research Center, University of California, Berkeley, CA, USA.
- Miller, D.J., Fahnestock, L.A. and Eatherton, M.R. (2011), "Self-centering buckling-restrained braces for advanced seismic performance", *Proceedings of ASCE Conference*, USA.
- Park, J., Lee, J. and Kim, J. (2012), "Cyclic test of buckling restrained braces composed of square steel rods and steel tube", *Steel Compos. Struct., Int. J.*, **13**(5), 423-436.
- Sabelli, R, Mahin, S.A. and Chang, C. (2003), "Seismic demands on steel braced-frame buildings with buckling-restrained braces", *Eng. Struct.*, **25**(5), 655-666.
- Tsai, K.C., Lai, J.W., Hwang, Y.C., Lin, S.L. and Weng, C.H. (2004), "Research and application of double-core buckling restrained braces in Taiwan", *13th World Conference on Earthquake Engineering*, Vancouver, Canada, November.
- Wang, C.L., Usami, T. and Funayama, J. (2012), "Evaluating the influence of stoppers on the low-cycle fatigue properties of high-performance buckling-restrained braces", *Eng. Struct.*, **41**, 167-176
- Wu, J., Liang, R.J., Wang, C.L. and Ge, H.B. (2012), "Restrained buckling behavior of core component In buckling-restrained braces", *Adv. Steel. Constr.*, **8**(3), 212-225.
- Zhu, S.Y. and Zhang, Y.F. (2008), "Seismic analysis of concentrically braced frame systems with self-centering friction damping braces", *J. Struct. Eng.*, **134**(1), 121-131.